Journal of Colloid and Interface Science 325 (2008) 558–566

Contents lists available at ScienceDirect

Journal of Colloid and Interface Science

www.elsevier.com/locate/jcis

Luminescent nanocrystals in phospholipid micelles for bioconjugation: An optical and structural investigation

Nicoletta Depalo [a,b], Antonia Mallardi [a], Roberto Comparelli [a], Marinella Striccoli [a], Angela Agostiano [a,b], Maria Lucia Curri [a,*]

[a] Istituto per i Processi Chimico Fisici (IPCF) CNR, sez. Bari, Via Orabona 4, 70126 Bari, Italy
[b] Dipartimento di Chimica, Università di Bari, Via Orabona 4, 70126 Bari, Italy

ARTICLE INFO

Article history:
Received 18 April 2008
Accepted 9 June 2008
Available online 13 June 2008

Keywords:
Colloidal nanocrystals
Luminescence
Phospholipids micelles
Dynamic light scattering
Bio-conjugation
Bovin serum albumine (BSA)
Nanocrystal functionalization

ABSTRACT

Organic capped luminescent CdSe@ZnS nanocrystals (NCs) have been incorporated in block copolymer micelles, formed by polyethylene glycol modified phospholipids (PEG lipids). The obtained water soluble NC including PEG lipid micelles have been conjugated with bovine serum albumine (BSA). The entire process has been investigated by using optical, structural and electrophoretic complementary techniques. Such an integrated approach has allowed to elucidate critical issues, such as the time and temperature effects on the phase behavior of the PEG lipid/NC aggregate structures, the emitting properties of the NCs before and after micelle formation and bio-conjugation and the effect of conjugation on the biological moiety. The overall results provide relevant insight on the fabrication of the bio-conjugates, on their stability and on preparative procedure reproducibility, in view of the use of the resulting protein decorated NCs as multifunctional hybrid building blocks for the fabrication of a variety of supramolecular assemblies to exploit in biological sensing and diagnostic applications.

1. Introduction

Currently one of the major challenge in materials chemistry is the synthesis of nanoscale structures with purposely designed properties. Indeed the emerging disciplines of nanoengineering, nanoelectronics, and nanobioelectronics require suitably sized and functionalized nanoparticles as "building blocks" for fabricating a new generation of innovative materials and solid-state devices. In this perspective, the unique size-dependent optical properties of semiconductor nanocrystals (NCs) make them extremely attractive component of multifunctional structures. Recent advance in chemical synthesis allows to synthesize colloidal NCs soluble in organic solvent, composed of a inorganic crystalline semiconductor heart coated by a protective shell of surface coordinating molecules, in a wide range of compositions with an excellent control on size, shape and crystallinity [1–5]. Moreover, their surface chemistry can be conveniently manipulated to promote their water solubility and to enhance compatibility with biological environments.

Nanoparticles share the same size regime (<50 nm) as that of many bio-molecules and can be used as *in vivo* or *in vitro* sophisticated fluorescent probes for cell imaging or bio-technologic assay applications [6–9]. Colloidal NCs have several peculiar advantages over conventional organic dyes typically used in optical bio-detection, as wide band absorption, narrow and tunable emission spectrum and high resistance to photobleaching phenomena [6,10].

Appropriate biological macromolecules, such as nucleic acid, proteins or anti-bodies, can be put into contact with inorganic NCs, thus merging the biochemical functionalities and the distinctive size-dependent chemical and physical properties of the two moieties. The resulting hybrid materials, characterized not only by their original properties, but also by an increasing degree of complexity, can be used as building elements of spatially and/or topologically organized nanoparticle superstructures, where the desired features and functions can be purposely conveyed [11,12].

A key point for the efficient use of NCs in all these fields of applications requires their aqueous solubility and their biocompatibility. Several studies have recently reported procedures to achieve these characteristics, while keeping intact their original optical features [6,13–17].

The most common strategy relies on exploiting hydrophobic interactions between the pristine NC capping layer and suitable amphiphilic molecules. Commercially available amphiphilic polymers bearing hydrophobic alkyl side chains and hydrophilic groups, such as poly(ethyleneglycol) (PEG) or multiple carboxylate groups, have been used [18–20]. A successful example of surface modification method through hydrophobic interaction, resulting in interdigi-

* Corresponding author. Fax: +39 080 5442128.
E-mail address: lucia.curri@ba.ipcf.cnr.it (M.L. Curri).

0021-9797/$ – see front matter
doi:10.1016/j.jcis.2008.06.018

tated structures, is represented by PEG modified phospholipid micelles encapsulating semiconductor NCs [15,21,22].

There is an increasing interest on the influence of the in water solubilization procedure on the overall diameter of NC/micelle system. After stabilization in aqueous solution and after a further addition of bio-molecules, a significative increase of the complex size can be observed. This seems to be a crucial point for a further employment of bio-conjugates in fields of application such as bio-sensing or bio-imaging [23,24].

Here trioctylphosphine oxide (TOPO) capped CdSe@ZnS NCs have been incorporated in PEG lipid micelles and the effect of the temperature and time on the hydrodynamic size of NC/PEG lipid micelles by means of dynamic light scattering (DLS) is reported [25–27]. Subsequently, the NCs/micelles complexes have been bio-conjugated with bovine serum albumine (BSA), a widely investigated protein which has been used as a convenient model for fundamental studies on protein/NC conjugates [25]. The entire process has been thoroughly monitored by using optical, structural and electrophoretic techniques, starting from the preparation of the bare micellar system, to the incorporation of NCs therein and, finally, to the bio-conjugation of the NCs.

The established BSA/NC conjugation provided an extremely reliable protocol which could be profitably used to further bind a variety of organic molecules to different protein functional sites, thus making the protein decorated NCs convenient hybrid building blocks for the fabrication of a variety of supramolecular assemblies [26–28] as well as for their use in bio-labelling and optical sensing.

2. Experimental

2.1. Materials

All chemicals were purchased of the highest purity available and were used as received without further purification or distillation. Cadmium oxide (CdO, powder 99.5%), selenium (Se, powder 99,99%), oleic acid (OLEA, technical grade 90%), trioctylphosphine oxide (TOPO, 99% and technical grade), tributylphosphine (TBP, 99%), trioctylphosphine (TOP, technical grade), diethylzinc (1.0 M solution in heptane) and hexamethyldisilathiane were purchased from Aldrich. Hexadecylamine (HDA) was purchased from Fluka. Bovine serum albumin (BSA) and the reagent grade salts for the 10 mM phosphate (PBS) and 1 M Tris (hydroxymethyl) aminomethane hydrochloride (Tris-HCl) buffer solutions at pH 7.4 were purchased from Sigma.

1,2-Dipalmitoyl-*sn*-glycero-3-phosphoethanolamine-*N*-[methoxy (polyethylene glycol)-2000] (16:0 PEG-2-PE), 1,2-distearoyl-*sn*-glycero-3-phosphoethanolamine-*N*-[carboxy(polyethylene glycol)-2000] (DSPE-PEG(2000) carboxylic acid) and 1,2-dipalmitoyl-*sn*-glycero-3-phosphocholine (16:0 DPPC) were purchased from Avanti Polar Lipids.

1-Ethyl-3-(3-dimethylaminopropyl) carbodiimide hydrocloride (EDC) and *N*-hydroxysulfosuccinimide (Sulfo-NHS) were purchased from Pierce. Tris-HCl precast gel (4–15% linear gradient) for polyacrylamide electrophoresis and Comassie Brilliant Blue R-250 were obtained from BIO-RAD. Bromophenol blue, β-mercaptoethanol, glycine and sodium dodecyl sulfate (SDS) were purchased from Sigma–Aldrich.

All solvents used were of analytical grade and purchased from Aldrich. All aqueous solutions were prepared by using water obtained by Milli-Q Gradient A-10 system (Millipore, 18.2 MΩ cm, organic carbon content $\leqslant$4 μg/L).

2.2. Synthesis of CdSe core NCs

Monodispersed CdSe NCs were synthesized by using the method reported by Qu et al. [29]. Briefly, OLEA and CdO were heated under vacuum, to obtain a colorless clear solution. At room temperature, TOPO (99%) and HDA were injected into the flask and, after a further treatment of degassing, the mixture was heated. The pure TBP and Se powder were dissolved in TBP initiate the nucleation, generating after 10 min CdSe NCs of about 3.5–4 nm in size. The synthesis was then stopped by rapidly cooling the flask and adding methanol. The obtained CdSe NCs were purified by repeated centrifugation, after precipitation with methanol, and re-dissolution in chloroform. The NC concentration was evaluated by absorbance spectra calculating the extinction coefficient as reported elsewhere [30].

2.3. Synthesis of CdSe@ZnS core–shell NCs

TOPO coated CdSe@ZnS core–shell NCs were prepared according to procedure reported by Reiss and coworkers [31]. Briefly, a chloroform solution of CdSe NCs (60 mg/mL) was injected into a flask, containing previously degassed TOPO (technical grade) and TOP. After the chloroform evaporation, the mixture was heated at 150 °C. Then, several drop-wise injections of a freshly prepared TBP stock solution, containing diethylzinc and hexamethyldisilathiane, were done. After the addition, the core–shell NCs were annealed at 90 °C and left stirring for few hours. Finally, the solution was cooled at room temperature and highly luminescent CdSe@ZnS NCs were isolated and purified by centrifugation after precipitation with methanol, and finally dissolved in chloroform.

2.4. Encapsulation of the CdSe@ZnS core–shell NCs in PEG lipid micelles

In a typical preparation, 2×10^{-7} mol of CdSe@ZnS core–shell NCs and 5.5×10^{-6} mol of phospholipids, containing 80% 16:0 PEG-2-PE and 20% DSPE-PEG(2000) Carboxylic Acid, were co-dissolved in chloroform [21]. After the solvent evaporation under nitrogen gas stream, a dried NC/PEG lipid layer was obtained. The film was kept under vacuum for 1 h, heated at 80 °C for 1 min and consequently hydrated with PBS buffer, pH 7.4 (1 mL). In order to obtain optically clear solutions, the samples were let to equilibrate at 80 °C for 20 min with periodic vigorous mixing and were subsequently kept at room temperature for 20 min before repeating the thermal cycle (4 times) [32]. Subsequently larger lipid aggregates were pelleted in a centrifuge (13,000 rpm for 5 min). The surnatant was recovered, filtered by using 0.2 μm filters and preserved at 60 °C until the bio-conjugation reaction. Empty PEG lipid micelles were prepared following the same protocol and omitting the NC addition. Should be noted that, throughout the preparation, both empty PEG lipid micelles and NC/PEG lipid micelles were repeatedly heated to 80 °C and subsequently cooled to room temperature. Remarkably, without such heating cycles only cloudy suspensions of large aggregates were obtained.

2.5. Bio-conjugation of the micelles with BSA

The bio-conjugation of BSA protein with NC micelles was performed by following a procedure reported in literature [33]. All steps were performed in PBS buffer pH 7.4 at room temperature. A freshly prepared CdSe@ZnS core shell NC/PEG lipid micelle suspension (CdSe@ZnS NC concentration $\sim 2 \times 10^{-6}$ M) was kept at room temperature for about 2 min and then mixed with freshly prepared EDC and Sulfo-NHS solutions, resulting in a final concentration of 0.05 M and 5 mM, respectively. BSA protein (2 mg/ml) was added and the mixture was gently stirred for 2 h. 30 mM Tris-HCl buffer solution was then used to quench the un-reacted Sulfo-NHS and stop the reaction. The BSA conjugated NC micelles were collected by ultracentrifugation (200,000*g*) and the conjugate containing pellet was washed with PBS buffer to completely

remove un-reacted cross-linker molecules, quenching agent and free BSA.

2.6. UV–vis and emission spectroscopy

Absorption measurements were performed by means of a UV/VIS/NIR Cary 5 Spectrophotometer (Varian). The photoluminescence (PL) spectra were recorded by using the Eclypse Spectrofluorimeter (Varian). The optical measurements on NC solutions were carried out at room temperature on the solution obtained directly from synthesis without any size sorting treatments. NC micelles before and after bioconjugation were investigated in PBS buffer at room temperature.

The relative PL quantum yields of NCs in solution were estimated by using Rhodamine 6G as dye reference and comparing the integrated PL intensity of the NCs and the dye, both recorded exciting solutions of same absorbance (<0.1 au, in order to minimize possible re-absorption effects), as reported elsewhere [34].

2.7. Time resolved photoluminescence spectroscopy

To investigate the fluorescence decay, the technique of time-correlated-single-photon-counting (TCSPC) was used. The NC solutions were excited by a pulsed picosecond (80 ps) laser diode (NanoLED 375L), operating at a wavelength of 375 nm and a repetition rate of 1 MHz. The obtained emission was focalized on the slit of a double monochromator and detected by a photon counting photomultiplier module (TBX from Horiba Jobin Yvon). The signal was timed by a time amplitude converter, digitized and sent to a multi-channel-analyzer. After deconvolution of the instrumental response, the PL decay signal was then analyzed applying a fitting procedure, in order to extract the radiative lifetime. The non-single exponential decay measurements were best fitted by using stretched exponential fitting functions, weighted with the radiative rates [35]. Such method has the advantage, with respect to previously used best-fitting models, to render readily available the information on physically interpretable rates.

2.8. FT-IR spectroscopy

Mid-infrared spectra were acquired with a Perkin–Elmer Spectrum One FTIR spectrometer equipped with a DTGS (deuterated tryglicine sulfate) detector. The spectral resolution used for all experiments was 4 cm^{-1}. For ATR measurements the internal reflection element (IRE) used was a three bounce 4 mm diameter diamond microprism. Cast films have been prepared directly onto the internal reflection element, by depositing the solution of interest (3–5 μL) on the upper face of the diamond crystal and allowing the solvent to evaporate.

2.9. Dynamic light scattering

Dynamic light scattering measurements were performed using the instrument Zetasizer-Nano S from Malvern. A 4 mW He–Ne laser (633 nm wavelength) with a fixed detector angle of 173° was used (non invasive backscattering). The time autocorrelation function (ACF) of scattered light intensity was converted into the ACF of scattered electric field. From this last quantity, the software supplied by the producer evaluates the intensity size distribution function through numerical Laplace inversion (CONTIN algorithm) [36] and subsequent application of Stokes–Einstein equation.

2.10. Gel electrophoresis

SDS-PAGE was performed on 4–15% gradient Tris-HCl precast gel according to the method of Laemmli [37]. Samples were heated at 80 °C for 10 min before running. Gels were characterized either as prepared, by detecting NCs luminescence by a DOC SYSTEM scanner from BIO-RAD, and after staining with Coomassie Blue.

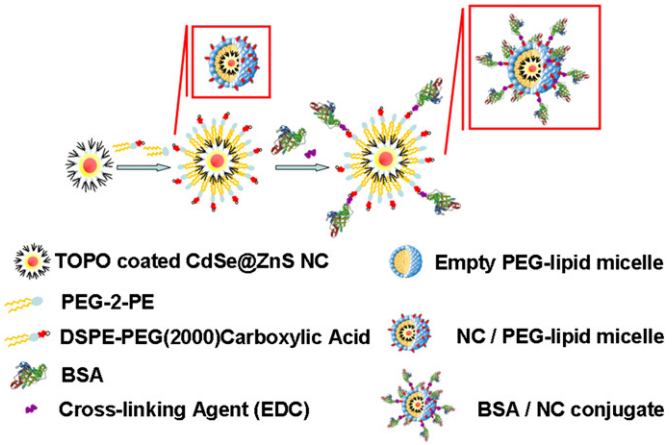

Chart 1. Proposed mechanism for NC micelle and BSA/NC conjugate formation.

2.11. Transmission electron microscopy

Transmission electron microscopy (TEM) images were obtained using JEOL 1100 microscope operating at 200 kV. The samples for the analysis were prepared by dropping dilute solutions of CdSe@ZnS NCs or NC/micelle suspensions onto 400-mesh carbon-coated copper grids and leaving the film to dry. The samples demonstrated to be stable under the electron beam, without degradation phenomena occurring within the typical observation times.

3. Results and discussion

In Chart 1 the scheme describing the steps of the experimental procedure carried out to prepare the BSA/NC conjugate system is shown. First, the TOPO coated CdSe@ZnS NCs have been embedded in the hydrophobic core of PEG lipid micelles. Then the micelles, functionalized with a carboxylic acid group, have been conjugated with BSA, enabling the formation of amide bond between the NC/PEG lipid micelles and the primary amine groups of the BSA.

In the first part of this work, the PEG lipid micellar systems have been prepared and utilized in order to achieve the solubilization of CdSe@ZnS NCs in aqueous solution.

Here, DLS technique have demonstrated to provide an accurate characterization of the obtained NC/PEG lipid complex. The DLS results have highlighted the complexity of the studied system and demonstrated that the micelles are significantly perturbed in geometry and size upon NC encapsulation. The spectroscopical characteristics of NCs have been monitored by means of UV–vis absorption and photoluminescence before and after encapsulation.

The second step of the work has been devoted to the set up of a bio-conjugation reaction between NC/PEG lipid micelles and BSA and a set of techniques have been used to confirm the successful NC conjugation.

In addition, time resolved photoluminescence measurements confirm that the conjugation with BSA does not significantly affect the intrinsic recombination process decay of the NCs in micelles and their optical properties.

3.1. NC encapsulation in lipid aggregates

The NC optical properties before and after transfer in the aqueous medium have been investigated by UV–vis and photolumi-

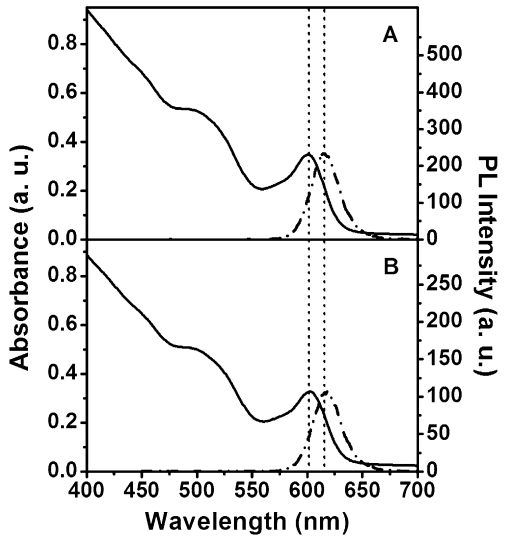

Fig. 1. Absorption (solid line) and photoluminescence (dashed/dotted line) spectra of CdSe@ZnS core shell NCs in chloroform solution (A) and after encapsulation in phospholipid micelles and re-dispersion in PBS (B). The two vertical dashed lines (eye guide only) across the two diagrams point out that no shift is detectable after the micelle formation.

nescence (PL) spectroscopies. In Fig. 1A the absorbance and PL spectra of NCs in their native solutions are shown. The spectra are dominated by a strong excitonic peak, indicating the narrow size distribution of the prepared NCs. Interestingly the encapsulation of the CdSe@ZnS core–shell NCs in PEG lipid micelles does not seem to significantly alter the NC optical properties (Fig. 1B). In particular, the spectral position and the width of the absorbance maximum remain unchanged, thus suggesting that no aggregation occurs, also in aqueous solution (Fig. 1B, solid line). Photoluminescence measurements indicate that even though the water environment induces a 50% decrease of NC emission (Fig. 1B, dash–dot line), the CdSe@ZnS NCs are still luminescent, probably thanks to an efficient coverage of the NC surface, ultimately resulting from the hydrophobic interactions between the TOPO layer and the alkyl chains of PEG lipids. In particular the PL quantum yield, relative to the Rhodamine 6G, moves from the value of 45% measured for NCs in their native chloroform solution to the value of 24% measured after the encapsulation in the micellar system.

In Fig. 2, the HRTEM images of the CdSe@ZnS core–shell NCs in organic solvent and upon incorporation in micelles are reported. The high resolution image (Fig. 2A) shows the high crystallinity of the spherical NCs, measuring about 4–5 nm of diameter, deposited on the TEM grid. Fig. 2B displays HRTEM image of the NC after incorporation in PEG lipid matrix and demonstrate how such structures maintain the same size and are still completely separated, thus proving the evidence that no NC aggregation phenomena occurred. The same conclusion can be drawn by the indirect size calculation performed by using spectroscopic measurements [30], which confirm the microscopical analysis. The DLS analysis has been then performed in order to investigate the hydrodynamic diameter (D_H) of hydrophobic NCs and of both empty and NC encapsulating micelles.

DLS measurements on TOPO capped hydrophobic NCs have resulted in a D_H of about 9 nm (data not shown), appreciably larger of that provided by HRTEM measurements (4–5 nm). A similar trend is reported from Pons et al. for NCs capped with various hydrophilic surface coatings [24]. The authors found that, for all nanoparticles investigated, the hydrodynamic size was consistently larger than the geometric size measured by TEM. In the case of the TOPO capped NCs used in this work, the difference in dimension can be accounted for by the presence of the TOPO capping agent layer on NC surface (∼1 nm) [38] and of the solvent shell [39,40], that contribute to increase the actual hydrodynamic size of the structures in solution.

Fig. 3A shows the size distribution of empty PEG lipid micelles obtained according the procedure reported in the experimental section. An unimodal population of small aggregates has been detected, revealing a D_H of about 12 nm and a narrow size distribution. Such investigated aqueous micelle suspension has been found stable for several days at 25 °C and also at higher temperatures (not shown), without any change in size and size distribution. These results are in excellent agreement with the data reported by Johnsson et al. for the same system [32,41].

The DLS measurements carried out at room temperature on a micellar sample immediately after the NC encapsulation demonstrated the presence of micellar aggregates with a D_H of 35 nm (Fig. 3B). The observed increase in the measured hydrodynamic diameter with respect to that of both hydrophobic NCs (9 nm) and empty micellar system can reasonably account for the presence of a lipid shell surrounding the NCs. This coating could result from the interdigitation of the hydrophobic tails of the TOPO molecules with those of PEG lipid molecules. Surprisingly, DLS measurements performed after storing the sample at room temperature have revealed the appearance of a new size peak corresponding to NC/PEG lipid aggregates with a larger hydrodynamic diameter. Therefore an investigation on the stability of the micellar system incorporating NCs has been considered necessary and accordingly performed.

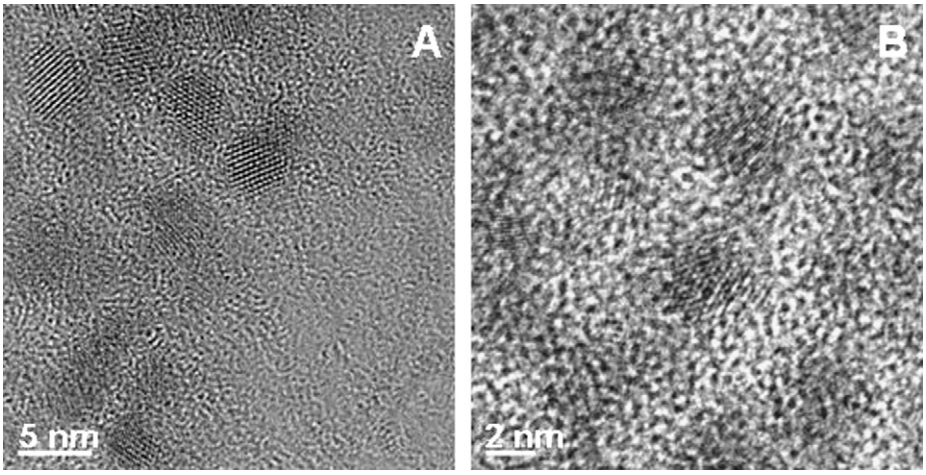

Fig. 2. HRTEM pictures of the CdSe@ZnS NCs before (A) and after (B) PEG lipid encapsulation. Sample stored for 7 h at room temperature.

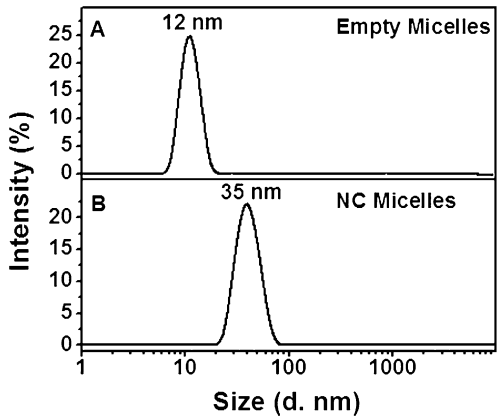

Fig. 3. Size distribution of empty PEG lipid micelles (A) and freshly prepared NC micelles (B), both in PBS buffer at pH 7.4.

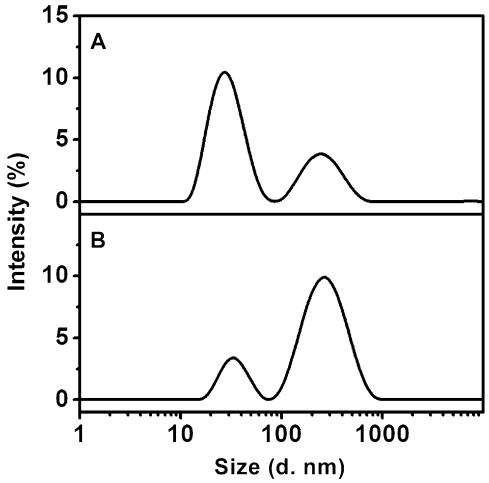

Fig. 4. Size distribution of NC/PEG lipid aggregates stored at 25 °C, after 7 (A) and 24 h (B) from preparation.

In particular the effects of experimental parameters, such as time and temperature, on the NC/PEG lipid aggregate size stability have been then studied, by means of DLS.

Fig. 4A shows the size distribution relative to the same sample of Fig. 3B, stored for 7 h at 25 °C. A bimodal size distribution is clearly evidenced: small aggregates with a hydrodynamic diameter of about 35 nm (consistent with that measured immediately after preparation) coexist with larger aggregates with a hydrodynamic diameter of about 250 nm. The fraction of large aggregates increases at the expense of small ones, the larger aggregates becoming the relevant population after 24 h at 25 °C, while the smaller size peak progressively reduces (Fig. 4B). Accordingly, storage of samples at low temperature allows the formation of large NC/PEG lipid aggregates in equilibrium with micelles.

No significant modifications in the size distribution have been observed when the temperature has been increased from 25 to 50 °C. Above 50 °C, a decrease in the mean size of the large aggregates and a parallel increase of the small aggregate population have been recorded. In Fig. 5A the relative amount (in terms of area of the peak, which accounts for the size distribution) of the small and the large aggregates are reported. In particular, at high temperature (80 °C) the complete disappearance of the peak corresponding to the large aggregates has been observed. In addition, after an equilibration time of 3 h at 80 °C, only one narrow peak has been detected, with a diameter of 20 nm for the corresponding micellar system (Fig. 5B).

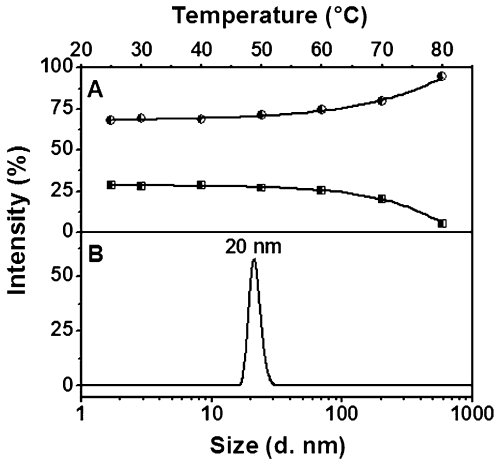

Fig. 5. Temperature dependence of NC/PEG lipid aggregate size. (A) Bimodal distribution depending on the temperature: intensity of size distribution for the narrow (circle) and the broad (square) peak. (B) Size distribution of NC micelles recorded at 80 °C after an equilibration time of 3 h.

Cooling back to 25 °C, such monodisperse sample reverts to the equilibrium situation between large and small aggregates above described. The coexistence between micelles and other self-assembled structures, both encapsulating NCs, has been also supported by TEM measurements performed on the same sample at room temperature. This structural investigation, probing mainly the size of the inorganic core, has shown several macro-aggregates of NCs, embedded in lipids, rather polydisperse in size with a diameter ranging from 30 to 200 nm (see SI). The NCs contained in all such structures are still well separated and do not undergo any aggregation, as demonstrated by HRTEM data (Fig. 2B).

These results point out the greater complexity of NC encapsulating PEG lipid micelles compared to the empty PEG lipid micelles.

It is generally accepted that PEG lipids at room temperature form spherical micelles in dilute aqueous solutions, also if a heating step up to 60 °C has been found necessary to obtain such kind of geometry [32,41]. Moreover, some papers report, at low and moderate temperature, the presence of lamellar aggregates or disks [42]. However, the effect of NC encapsulation on size stability of such system is not still extensively documented. Dubertret et al. reported a diameter between 10 and 15 nm for CdSe@ZnS containing micelles. This size was estimated only by TEM measurements on micelles made of a DPPC/PEG(2000)DSPE mixture showing the presence of monodisperse micelles [21]. Pons et al. reported a DLS study on NCs capped with different hydrophilic surface ligands. The authors discussed the effects of surface coatings on nanoparticle hydrodynamic size and the difference between information obtained from DLS and heavy atomic techniques. Moreover they pointed out the relevance of NCs hydrodynamic dimension for their performance in imaging and biological assays [24].

In our work, the attention has been focused on the NC/PEG lipid system. Our DLS data reveal a complexity for NC encapsulating PEG lipid micelles never described before. In fact, at lower temperatures, a true equilibrium between small spherical micelles and large polidisperse aggregates has been found. These aggregates are very large (about 250 nm in hydrodynamic diameter) and such a large size can be hardly accounted for by a spherical shape. A 250 nm diameter sphere implies a volume of about four hundred fold the volume of NC encapsulating small micelles ($D_h = 35$ nm). Tacking into account the high density of NCs, aggregates of this size should give rise to an observable sedimentation. On the contrary the solution remains stable for days. Mono- or two-dimensional aggregates (rods or disk) are more likely to form

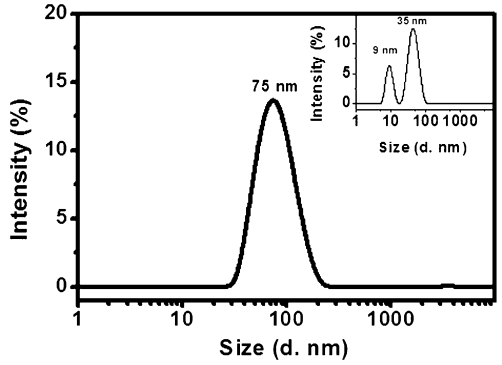

Fig. 6. Size distribution of BSA/NC conjugates. Inset: Size distribution of a mixture of NC micelles and BSA.

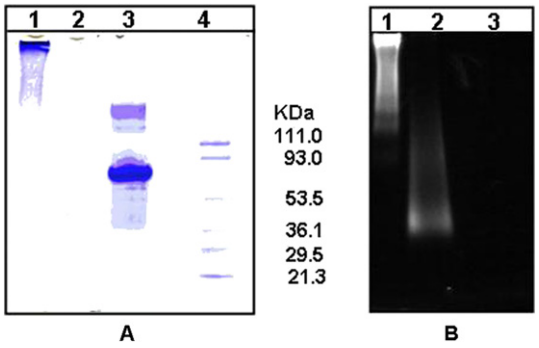

Fig. 7. BSA conjugation of NC/micelles. The three lanes correspond to bioconjugate NC micelles (lane 1), free NC micelles (line 2), BSA standard protein (lane 3). A standard protein ladder was also added in the gel (lane 4). The left panel is the image obtained after staining the gel with Coomassie Blue and the right panel is a fluorescence image of the same plate.

since in these cases a high hydrodynamic diameter corresponds to a considerably smaller volume.

The presence of NCs in the micellar system could induce a change in the packing parameter of PEG lipids and at low temperature a lateral fusion of micelles can occur with the formation of larger aggregates. A high polydispersity in dimensions is expected for these structures [43].

It has also been observed that upon warming up to 80 °C the aggregates disappear and highly monodisperse NC/micelles of 20 nm of diameter have obtained. The observed equilibrium and the temperature dependence are reversible. Such behavior has not been observed for empty PEG lipid micelles. The presence, at high temperature, of monodispersed spherical micelles suggests a decrease of the packing parameter at 80 °C thus favoring an high curvature of the lipidic film. On the contrary at room temperature, the above reported data hint an higher packing parameter consistent with the presence of locally cylindrical or lamellar aggregates. Since the conformation of either the lipidic (PE and DSPE) either the ethoxylate (PEG) moieties of the surfactants are known to depend on the temperature, an influence of the temperature on the packing properties DSPE-PEG is reasonable [44].

The reported data represent a considerable advance in the NC encapsulation protocol. Indeed, the availability of a monodisperse distribution in size of NC/PEG lipid aggregates is a crucial point for obtaining monodisperse bio-conjugate structures, and this is of critical importance for their further employment in bio-sensing and bio-imaging applications.

3.2. Conjugation of NC/PEG lipid micelles with BSA

On the basis of obtained information, the bio-conjugation process of BSA protein with NC/PEG lipid micelles has been performed only starting from freshly prepared samples and immediately after filtration, when a monomodal size distribution is still present.

The bio-conjugation has been carried out using a 20% of PEG lipids functionalized with a carboxylic acid group bound to PEG moiety, which can thus enable the formation of amide bonds between the NC/PEG lipid micelles and the primary amine groups of the BSA. Namely BSA has been covalently bound to NC/PEG lipid micelles by using the sulfo-NHS and EDC reaction, according to the procedure reported in literature [33].

The effect of the cross-linking reaction with BSA on the hydrodynamic diameter of the NC/PEG lipid systems has been monitored by means of DLS, as reported in Fig. 6. An increase of NC/micelle/BSA complex average diameter to about 75 nm has been recorded, thus supporting the occurrence of the BSA conjugation with the NC containing micelles (Fig. 6). In order to exclude any non specific absorption of BSA on NC/PEG lipid micelle surface, the size distribution of a mixture containing freshly prepared NC/micelles and BSA, without any linkers, has been measured. The result is reported in the inset of Fig. 6, that shows two distinct peaks, ascribable to the free BSA (9 nm) and the NC/PEG lipid micelles (35 nm). Accordingly, it is possible to conclude that the increase in diameter of the NC/PEG lipid micelle based systems has occurred only when a chemical reaction with BSA was possible.

The obtained BSA/NC conjugates have been stored at room temperature and their size distribution monitored by means of DLS over a week. A monomodal distribution remains present without any increase in diameter. BSA covalent conjugation with NC/PEG lipid micelles thus act for preventing the aggregation at room temperature, since the bio-conjugation is able to “freeze” the equilibrium between the two aggregated forms, resulting in the occurrence of only the smaller structures. Furthermore, after one week, a slightly increase in hydrodynamic diameter is observed, but this can be reasonably accounted by an unfolding process of BSA moiety due to its ageing.

The covalent conjugation of NC micelles to BSA has been confirmed by SDS-PAGE analysis. Two different imaging modes have been used to characterize the same gel after the run, and thus verify the coupling reaction. Fig. 7A shows the Coomassie Blue stained image of SDS-PAGE electrophoretic results for BSA/NC conjugates (well 1), free NC/PEG lipid micelles (well 2), free BSA (well 3) and standard proteins (well 4). The Coomassie Blue stains specifically proteins, accordingly free NC micelles can not be detected by this staining assay (lane 2).

In the lane 3 a band corresponding to about 66 KDa, relative to free BSA, is clearly evidenced. After the conjugation, the BSA band shifts from 66 KDa to a higher apparent molecular mass (lane 1). Such a delay in the band run could be explained with the increase in size of BSA/NC conjugates with respect to the free BSA. The bioconjugates can enter into the gel, while the overall run throughout the matrix is not possible anymore due to the mass increase. No band corresponding to free BSA could be detected in the lane 1, thus suggesting the effectiveness of the conjugation procedure (see Section 2).

It is worthwhile to notice that the CdSe@ZnS NC fluorescence is still detectable after the electrophoretic run, thus providing a useful test to prove the conjugation. In Fig. 7B, the luminescence image of the same gel (taken before Coomassie staining), clearly shows a strong luminescence from the band of bio-conjugated NCs (lane 1). In lane 2 a luminescent band relative to free NC micelles, absent in lane 1, is clearly evidenced in the lower part of the gel thus confirming the mass increase of NC aggregates after BSA conjugation, while no detectable signal is recorded from the free BSA (lane 3). SDS-PAGE provides only a qualitative analysis and does not allow to make an accurate evaluation of the molecular masses of the highly charged NC/PEG lipid micelles and of their bio-conjugates. In this case the mobility is strongly affected by the

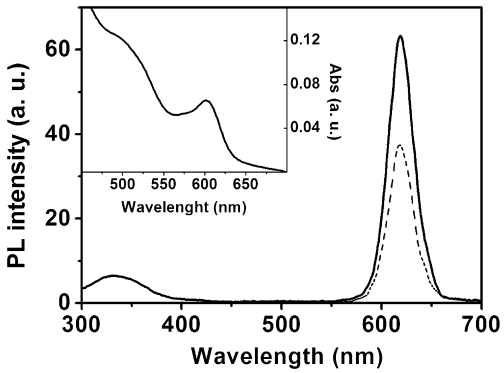

Fig. 8. Photoluminescence spectra of BSA/NC conjugates recorded at two different excitation wavelengths: 270 nm (solid line) and 400 nm (dashed line). Inset: Absorbance spectrum of BSA/NC conjugates.

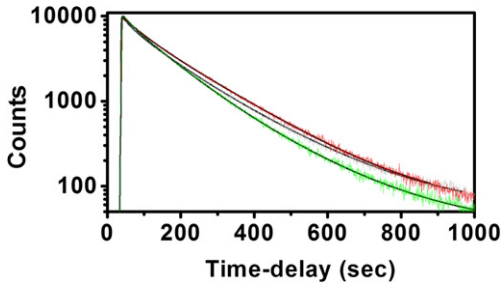

Fig. 9. Time-resolved photoluminescence decay curves from CdSe@ZnS core shell NCs in chloroform solution (green line), NC micelles (red line) and BSA/NC conjugates (grey line). (For interpretation of the references to color in this figure legend, the reader is referred to the web version of this article.)

charge density, which can be dramatically different in the micelles and in the bio-conjugates [33,35].

The photoluminescence and absorption spectra of BSA/NC conjugates have been reported in Fig. 8. The PL spectrum (registered at $\lambda_{exc} = 270$ nm) shows the contemporary presence of a broad band centered at 330 nm and a narrow band centered at 640 nm, attributable to BSA and NCs, respectively. The observed fluorescence in the range 280–430 nm ascribed to BSA is due to the presence of two tryptophan residues, located in the hydrophobic protein domains [25]. The emission at 640 nm is clearly due to the intrinsic recombination in the semiconductor NCs. The same emission for NCs has been observed with an excitation light of 400 nm (dashed line). The bio-conjugated NCs exhibited the same absorption spectrum (shown in the inset) as hydrophobic NCs and NC/PEG lipid micelles (Fig. 1). It is clearly evident that, after conjugation process, the optical properties of CdSe@ZnS core shell NCs are still retained. In addition, a value of 25% for the relative PL quantum efficiency has been measured on the conjugated BSA/NC system, indicating that the BSA presence on micelle surface does not significantly perturb the NC emission.

The radiative decay dynamics of CdSe@ZnS NCs in non polar solvent, in PEG lipid micelles and in BSA conjugates have been measured with time resolved spectroscopy, as reported in Fig. 9. The experiments have been performed on samples originating from the same NC synthesis, in order to have comparable NC size distribution. In this way, any difference observed in the spectral behavior can be attributed only to changes in the organic shell and environment of the NCs. Two main characteristics are peculiar for the PL decay dynamics in NCs. First, the decay time of NCs (tens nanoseconds at room temperature) strongly differs from the decay time measured for CdSe bulk material. This long decay is attributed to the optically inactive low energy state, called “dark exciton state.”. The second peculiarity is the multi-exponential behavior

Table 1
Best-fit values for stretched exponential fit of the data shown in Fig. 9[a]

	τ_d (ns)	β	R^2
NCs	13.30 ± 0.02	0.77	0.99962
NC/micelles	16.50 ± 1.80	0.83	0.99409
BSA/NC micelles	17.10 ± 0.06	0.90	0.99168

[a] NCs—CdSe@ZnS core–shell NCs in chloroform solution, NC/micelles—NC micelles in aqueous solution, BSA/NC micelles—BSA/NC conjugates in aqueous solution, τ_d—decay time ± st. deviation, β—parameter quantifying how close the PL decay approaches the single exponential, R^2—goodness of the fitting.

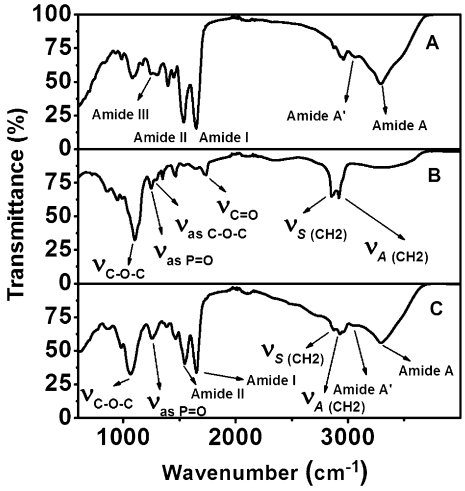

Fig. 10. FT-IR-ATR spectra of (A) pure BSA, (B) NC/micelles and (C) BSA/NC conjugates, all cast from PBS aqueous solution.

of both the ensemble of NCs and single NCs, due to local fluctuation of the electrostatic environment that also induces blinking phenomena. The PL decay measurements have been best fitted by using a stretched exponential model (Eq. (1)), weighted by radiative rates,

$$I(t) = Y_0 + C \cdot (\beta/t) \cdot \left((t/\tau_d)^{\beta}\right) \cdot \exp(-t/\tau_d)^{\beta} \quad (1)$$

in which τ_d is the decay time and β is a parameter that quantify how close the PL decay approaches the single exponential [45]. Value close to unit reveals pure mono exponential decay. The best fitting results are summarized in Table 1.

As can be clearly noticed in Table 1, an increase in recombination time can be measured for NCs incorporated in micelles with respect to what obtained for NCs in their native non polar solution. The decay time remains nearly the same after the conjugation of the NC/micelles system with the BSA, indicating that the micelle is effective in the protection of NC surface and that the conjugation process does not perturb the optical properties of the NC when embedded in the micelles. The high values obtained for β in the fitting procedure demonstrate a near single exponential kinetics dominated by the radiative lifetime of the single NCs.

An evaluation of the BSA protein structure has been performed before and after NC/PEG lipid micelle conjugation by means of a FT-IR analysis, in order to find out evidence of the bio-conjugation reaction and to detect possible modifications of polypeptide backbone and side-chain functional groups after conjugation with NC micelles.

Fig. 10 shows the spectra relative to (A) free BSA, (B) free NC/PEG lipid micelles, (C) BSA/NC conjugates. Moreover, the spectra relative to NCs in organic solvent and phospholipids and a summary of the absorption band frequencies of the investigated samples together with their assignments, are reported in SI.

The assignment of BSA vibrational bands (A) has been done taking into account that the infrared-active modes of the peptide

backbone are made as a function of the so-called *Amide* modes [46–48]. The N–H stretching is a localized mode and appears as a doublet represented by the Amide A and Amide A′ bands at 3290 and 3062 cm^{-1}, respectively. The Amide I and II bands have been found to have maximum peaks at 1650 and 1540 cm^{-1}. The Amide I mode is primarily ascribed to the C=O stretching band, while the Amide II mode is attributed to an out-of-phase combination of largely NH in plane bending and CN stretching. The peaks at 1302 and 1246 cm^{-1} have been attributed to the more complex Amide III band, which is the in-phase combination of NH in-plane bending and CN stretching. Infrared active modes attributed to side-chain vibrations include C–H stretching modes at 2959, 2929 and 2872 cm^{-1}.

The overall data point out that the BSA fundamental and characteristic infrared modes have been mostly retained in the BSA/NC conjugate spectrum (C) which roughly corresponds to the sum of the free BSA spectrum and NC micelle spectrum (reported in B). Indeed the peaks of the Amide I, Amide II, Amide A modes are still presents. However a slight shift of about 7 cm^{-1} has been recorded for the Amide II modes (see SI, Table 1).

For the BSA/NC conjugates the Amide A′ mode results less intense than for the equivalent in the free BSA, being also shifted of about 16 cm^{-1}. The shape of the Amide III mode in the BSA shows also a modification in the wavenumber region between 1200–1350 cm^{-1}, when the BSA binds the NC micelles. Such a modification could be ascribed to its convolution with the peak centered at about 1250 cm^{-1}, associated with the lipid phosphate asymmetric stretching band, which is diagnostic for the microenvironment of the lipid headgroups [49–51].

In addition, in the BSA/NC conjugate spectrum the large peak corresponding to the C–O–C ether stretching, univocally ascribable to the PEG lipids, shows a not negligible shift of about 40 cm^{-1}, with respect to the same signal in NC/PEG lipid micelle (1100 and 1062 cm^{-1} for NC/PEG lipid micelles and BSA/NC conjugates respectively). Interestingly the same characteristic signal stays unchanged in free NC/PEG lipid micelle spectrum. This evidence accounts for an active participation of the C–O–C in the bio-conjugation reaction, while only no direct involvement can be seen in the NC micelle aggregate formation, where only the alkyl chains are interested.

The ensemble of data safely indicates that no significant modification occur in the peptide backbone structure, as well as in the side-chain functional groups, after BSA conjugation to NC containing micelles. While the occurrence of a successful bio-conjugation reaction is suggested by the shift of C–O–C stretching and modification of Amide A′ mode, both signs of the participation of carboxylic function of the PEG polymer to the reaction with the native amine group present in BSA protein.

4. Conclusions

A PEG lipid micellar system has been used to encapsulate and water solubilize hydrophobic CdSe@ZnS core–shell NCs. The original size dependent optical properties of NCs have demonstrated to be retained in the resulting aggregates. The optical investigation carried out by means of DLS has provided essential insights on the temperature and time stability of the obtained NC containing micelles. A structural evolution of NC/PEG lipid micelles has been provided by DLS technique, pointing out the complexity of this system.

The conjugation of the NC/PEG lipid micelles with BSA has successfully lead to fluorescent and stable hybrid system, as confirmed by photophysical and time resolved PL measurements.

DLS investigations performed on such bio-conjugates have proven that covalent binding of BSA to the micellar surface stabilizes the NC encapsulating system. This work represents a considerable improvement over the existing NC water solubilization and bio-conjugation protocol which can be used as a model system for protein/NC conjugation.

The huge potential of the proposed BSA/NC conjugate hybrid complex can be envisaged as a key structural building block for multi-color and multiplexing bio-probes detection, also exploiting molecular recognition processes. Finally the perspective of use such bio-conjugated building blocks for fabricating ordered architectures upon immobilization with suitable antibody systems can be seen as a preliminary step for NC-based bio-chip and bio-sensor development.

Acknowledgments

The authors grateful acknowledge Prof. G. Palazzo for the use of the DLS apparatus and the valuable discussion of the DLS measurements, Prof. R. Tommasi for the useful discussion on the time resolved photophysical characterization and Dr. G.C. Capitani for TEM measurements. This work has been partially funded by EC through project NaPa (Contract No. NMP4-CT-2003-500120) and by Italian MIUR SINERGY programme (FIRB RBNE03S7XZ).

Supporting information

The online version of this article contains additional supporting information.

Please visit DOI: 10.1016/j.jcis.2008.06.018.

References

[1] I. Lisiecki, J. Phys. Chem. B 109 (2005) 12231.
[2] S.M. Lee, S.N. Cho, J. Cheon, Adv. Mater. 15 (2003) 441.
[3] C. Burda, X. Chen, R. Narayanan, M.A. El-Sayed, Chem. Rev. 105 (2005) 1025.
[4] Y. Yin, A.P. Alivisatos, Nature 437 (2005) 664.
[5] F. Shieh, A.E. Saunders, B.A. Korgel, J. Phys. Chem. B 109 (2005) 8538.
[6] X. Michalet, F.F. Pinaud, L.A. Bentolila, J.M. Tsay, S. Doose, J.J. Li, S.G. Sundaresan, A.M. Wu, S.S. Gambhir, S. Weiss, In Vivo Imag. Diagnostics 307 (2005) 538.
[7] X. Wu, H. Liu, J. Liu, K.N. Haley, J.A. Treadway, J.P. Larson, N. Ge, F. Peale, M.P. Bruchez, Nat. Biotechnol. 21 (2003) 41.
[8] Q. Wang, Y. Kuo, Y. Wang, G. Shin, C. Ruengruglikit, Q. Huang, J. Phys. Chem. B 110 (2006) 16860.
[9] N.L. Rosi, C.A. Mirkin, Chem. Rev. 105 (2005) 1547.
[10] A.P. Alivisatos, Nat. Biotechnol. 22 (2004) 47.
[11] Z. Dai, A.N. Kawde, Y. Xiang, J.T. La Belle, J. Gerlach, V.P. Bhavanandan, L. Joshi, J. Wang, J. Am. Chem. Soc. 128 (2006) 10018.
[12] I.A. Banerjee, L. Yu, H. Matsui, Nano Lett. 3 (2003) 283.
[13] P.D. Cozzoli, T. Pellegrino, L. Manna, Chem. Soc. Rev. 35 (2006) 1195.
[14] J.A. Kloepfer, S.E. Bradforth, J.L. Nadeau, J. Phys. Chem. B 109 (2005) 9996.
[15] H. Fan, E.H. Leve, C. Scullin, J. Gabaldon, D. Tallant, S. Bunge, T. Boyle, M.C. Wilson, C.J. Brinker, Nano Lett. 5 (2005) 645.
[16] X. Gao, L. Yang, J.A. Petros, F.F. Marshall, J.W. Simons, S. Nie, Curr. Opin. Biotechnol. 16 (2005) 63.
[17] M.J. Meziani, P. Pathak, B.A. Harruff, R. Hurezeanu, Y.P. Sun, Langmuir 21 (2005) 2008.
[18] T. Pellegrino, L. Manna, S. Kudera, T. Liedl, D. Koktysh, A.L. Rogach, S. Keller, J. Radler, G. Natile, W.J. Parak, Nano Lett. 4 (2004) 703.
[19] X. Wu, H. Liu, J. Liu, K.N. Haley, A.J. Treadway, J.P. Larson, N. Ge, F. Peale, M.P. Bruchez, Nat. Biotechnol. 21 (2002) 41.
[20] X. Gao, Y. Cui, R.M. Levenson, L.W.K. Chung, S. Nie, Nat. Biotechnol. 22 (2004) 969.
[21] B. Dubertret, P. Skourides, D.J. Norris, V. Noireaux, A.H. Brivanlou, A. Libchaber, Science 298 (2002) 1759.
[22] G.Y. Shan, D. Li, L.Y. Feng, X.G. Kong, Y.C. Liu, Y.B. Bai, T.J. Li, J.Z. Sun, Chin. J. Chem. 23 (2005) 1688.
[23] R.A. Sperling, T. Liedl, S. Duhr, S. Kudera, M. Zanella, C.A.J. Lin, W.H. Chang, D. Braun, W.J. Parak, J. Phys. Chem. C 111 (2007) 11552.
[24] T. Pons, H.T. Uyeda, I.L. Medintz, H. Mattoussi, J. Phys. Chem. B 110 (2006) 20308.
[25] T. Peters, Biochemistry, Genetics, and Medical Applications, Academic Press, San Diego, 1996.
[26] M.J. Meziani, Y.P. Sun, J. Am. Chem. Soc. 125 (2003) 8015.
[27] E. Katz, I. Willner, Angew. Chem. Int. Ed. 43 (2004) 6042.
[28] J.L. Zhang , B.X. Han, J. Chen, Z.H. Li, Z.M. Liu, W. Wu, Biotechnol. Bioeng. 89 (2005) 274.

[29] L. Qu, X. Peng, J. Am. Chem. Soc. 124 (2002) 2049.
[30] W.W. Yu, L. Qu, W. Guo, X. Peng, Chem. Mater. 15 (2003) 2854.
[31] P. Reiss, J. Bleuse, A. Pron, Nano Lett. 2 (2002) 781.
[32] M. Johnsson, K. Edwards, Biophys. J. 85 (2003) 3839.
[33] S. Wang, N. Mamedova, N.A. Kotov, W. Chen, J. Studer, Nano Lett. 2 (2002) 817.
[34] I. Mekis, D.V. Talapin, A. Kornowski, M. Haase, H. Weller, J. Phys. Chem. B 107 (2003) 7454.
[35] A.F. van Driel, I.S. Nikolaev, P. Vergeer, P. Lodahl, D. Vanmaekelbergh, W.L. Vos, Phys. Rev. B 75 (2007) 035329(1).
[36] S.W. Provencher, J. Chem. Phys. 64 (1976) 2772.
[37] U.K. Laemmli, Nature 227 (1970) 680.
[38] I. Geissbuehler, R. Hovius, K.L. Martinez, M. Adrian, K.R. Thampi, H. Vogel, Angew. Chem. Int. Ed. 44 (2005) 1388.
[39] W. Jiang, S. Mardyani, H. Fischer, C.W. Chan, Chem. Mater. 18 (2006) 872.
[40] Malvern Instruments, Application note, http://azom.com./details.asp?ArticleID=2723.
[41] M. Johnsson, P. Hansson, K. Edwards, J. Phys. Chem. B 105 (2001) 8420.
[42] G. Blume, G. Cevc, Biochim. Biophys. Acta 157 (1993) 1146.
[43] J.N. Israelachvili, Intermolecular and Surface Forces. With Applications to Colloidal and Biological Systems, Academic Press, Harcourt Brace Jovanovich Publishers, London, 1985, chap. 16.
[44] D. Marsh, Chem. Phys. Lipids 57 (1991) 109.
[45] N. Mamedova, N.A. Kotov, Nano Lett. 1 (2001) 281.
[46] J.L. Burt, C. Gutierrez-Wing, M. Miki-Yoshida, M. Jose-Yacaman, Langmuir 20 (2004) 11778.
[47] J. Grdadolnik, Acta Chim. Slov. 50 (2003) 777.
[48] Y.S. Wei, S.Y. Lin, S.L. Wang, M.J. Li, W.T. Cheng, Biopolymers 72 (2003) 345.
[49] J.A. Richard, I. Kelly, D. Marion, M. Pézolet, M. Auger, Biophys. J. 83 (2002) 2074.
[50] A.V. Popova, D.K. Hincha, Glycobiology 15 (2005) 1150.
[51] I.J. Vereyken, V. Chupin, F.A. Hoekstra, S.C.M. Smeekens, B. de Kruijff, Biophys. J. 84 (2003) 3759.